Formation of Antarctic Bottom Water
Part II : Method and Tools

Culture Sciences
de l'Ingénieur

Noémie SCHIFANO, Alberto NAVEIRA-GARABATO,
Alessandro SILVANO, Farid BENBOUDJEMA

Published on :
June 2021

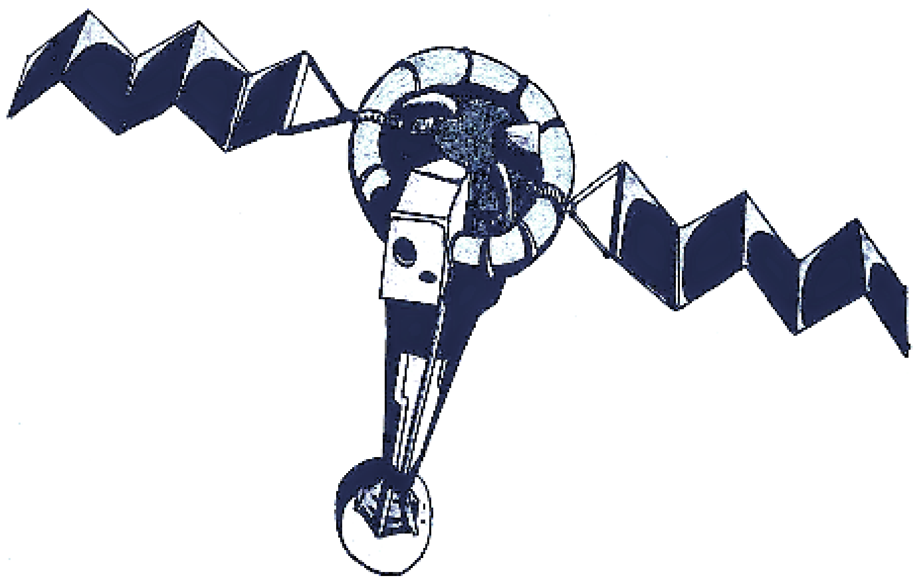

MPU, Cowboy Bebop

This document comes from a one-year internship at Southampton University (UK), with Prof Alberto NAVEIRA-GARABATO and Dr. Alessandro SILVANO. Noémie SCHIFANO is a final year student at Ecole Normale Supérieure Paris-Saclay. After a first-year master degree in civil engineering, she had pursued a second-year master degree in physical oceanography at Ecole Polytechnique.

Acknowledgments I would like to thanks Mr. Alberto NAVEIRA-GARABATO and Mr. Alessandro SILVANO for all the help they have provided me during this internship. I would also like to thanks Mr. Farid BENBOUDJEMA and Mrs. Hélène HORSIN-MOLINARO for making this publication possible.

Radar altimetry data were supplied by the European Space Agency (`https://earth.esa.int/web/guest/data-access/`) and GRACE data were supplied by the Jet Propulsion Laboratory (`https://podaac.jpl.nasa.gov/dataset/TELLUS_GRAC-GRFO_MASCON_CRI_GRID_RL06_V2`).
Argo floats data were collected and made freely available by the Coriolis project and programmes that contribute to it (`http://www.coriolis.eu.org/`) and NOAA (`https://www.nodc.noaa.gov/argo/floats_data.htm`). Mean Sea Level Pressure is from ECMWF (`https://cds.climate.copernicus.eu/cdsapp#!/dataset/reanalysis-era5-single-levels-monthly-means?tab=overview`).

Table of contents

1 Introduction

Oceans are the thermal regulators of the Earth : solar radiations warm up the ocean, whose heat storage capacity is much higher than that of the atmosphere and the land. Due to the spherical shape of the Earth, equatorial region accumulates more solar radiations than the poles. As the region close to the Equator receives the most solar radiations, a natural oceanic circulation, from the Equator to the poles, is set up. This circulation is the Meridional Overturning Circulation (MOC). The MOC is an important phenomenon for the biodiversity because it regulates the Earth thermal heating, but also because it transports nutrients, oxygen and carbon dioxide.

MOC is mostly composed by a surface circulation from the Equator to the Poles, and an abyssal circulation. When waters transported by the MOC reach the Poles, one part is transformed into the denser water due to surface cooling and brine rejection by sea ice formation. In those area, there is a huge density gradient, where denser water are at the surface of the Ocean. Therefore, heavy surface waters sink into the abyss : this is called "bottom water formation". Bottom water are the waters which transport oxygen, carbon dioxide and nutrients from the surface of the ocean and the atmosphere to the deep ocean.

Our knowledge about Antarctic Bottom Water (AABW) is limited, principally because of the difficulty to measure Antarctic water properties. Indeed, sea ice limits fieldwork. Campaigns are possible only in Summer, in specific area.

The purpose of this internship, topic of these publications, is to measure AABW formation using satellite data. The results are then compared with in−situ data (Argo floats and one mooring). A first document which presents state of the art knowledge of Antarctic physical oceanography and the issue of AABW formation, "Formation of Antarctic Bottom Water : General knowledge", has been published. How is it possible to measure antarctic bottom water formation using satellites? How can we know if satellites measurements are correct? What are all of these technologies? All of these points are detailed in this document. A third document, providing this internship results, will finally be published.

Writer's Note

In this document, many hand-written drawings and schematics are used. The purpose, by linking art and science, is to offer students another way of visualisation and, hopefully, a good understanding of physical processes.

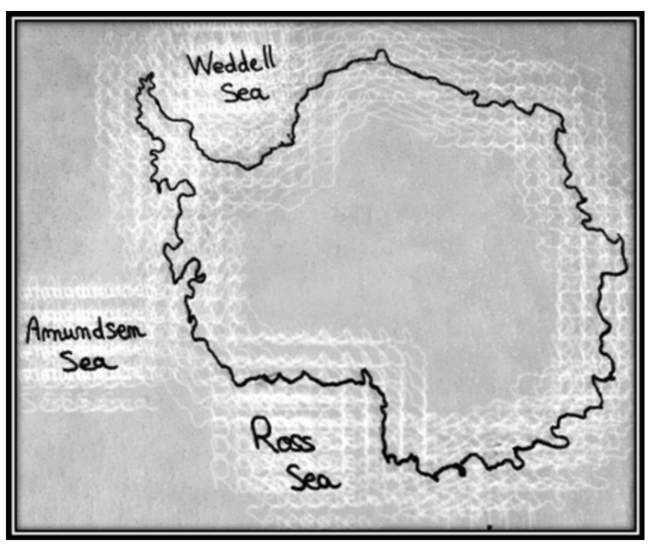

2 Measure of Antarctic Bottom Water by Satellite

2.1 How is it measured?

Changing in ocean volume can be due to changes in mass or density:

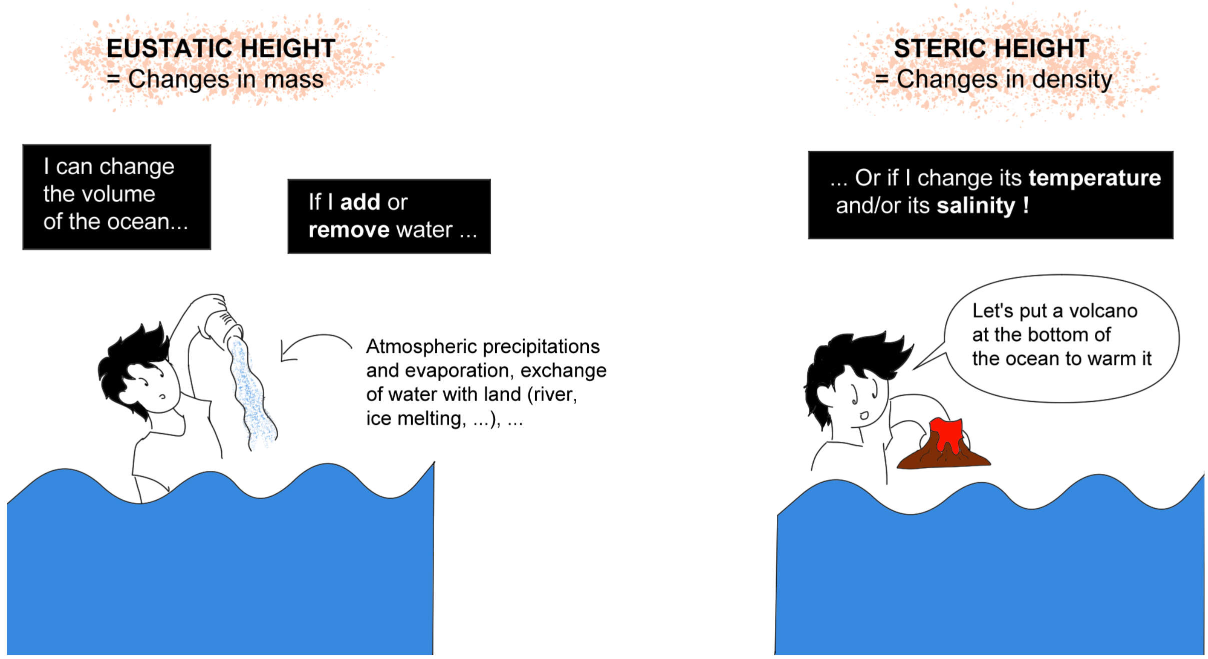

Steric height is what we aim to study to see AABW formation. Using satellite, the ocean total height anomaly (steric plus eustatic) and the eustatic height anomaly are known. Therefore, steric height anomaly may be computed:

Steric height anomaly = **Total height anomaly** (steric + eustatic)
Cryosat-2 and Envisat data

- (**Eustatic height anomaly**(changes in ocean mass)
GRACE data

- **Atmospheric pressure anomaly**)
ERA5 data

Nota bene: The weight of the atmosphere can change the height of the ocean. The weight of the atmosphere is measured through the atmospheric pressure : the bigger the atmospheric pressure, the heavier the atmosphere. That is why the atmospheric pressure anomaly is removed from the eustatic height anomaly.

2.2 How is the steric height anomaly interpreted?

A dense water column has a smaller steric height than a light water column. Indeed, light waters take up more space than dense waters. An increasing of density makes the water column shrink. Therefore, **a negative value of steric height anomaly means that means that density increases, enhancing AABW formation**. On the opposite, if the steric height anomaly is positive, freshwater content increases (fig. 1).

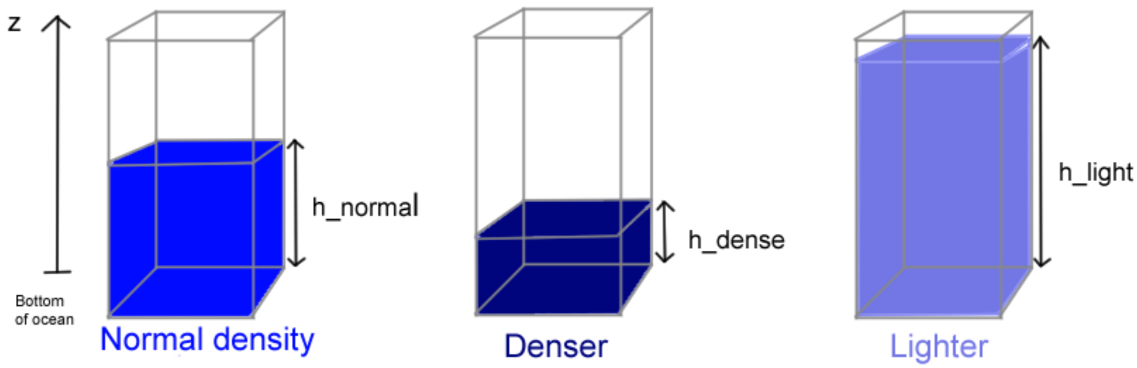

Figure 1: Link between density and height of a water column.

In Summary ...

The **more negative** the steric height anomaly is, the more Antarctic Bottom Water is formed.

On the opposite, the **more positive** the steric height anomaly is, the more **fresh water** accumulates.

3 CRYOSAT-2 and ENVISAT : Total ocean height

The total ocean height is determinated using satellites CRYOSAT-2 and ENVISAT.

3.1 Characteristics of those satellites

Both CRYOSAT-2 and ENVISAT have been launched by the European Space Agency (ESA), and have a Doppler Orbitography by Radiopositioning Integrated on Satellite (DORIS) receiver on them. DORIS is the system which allows those satellites to know their trajectory and their position relative to the Earth.

CRYOSAT-2

CRYOSAT-2 is 4.6 meters long, 2.34 meters wide and 2.2 meters high. It weighs **725 kg** (esa, cryosat). Its main mission is to measure ice-covering around the world, to study the impact of climate change on ice melting. To do so, SAR Interferometer Radar ALtimeter (SIRAL) has been implemented on CRYOSAT-2. SIRAL is made by Thales Alenia Space, in Toulouse (France).

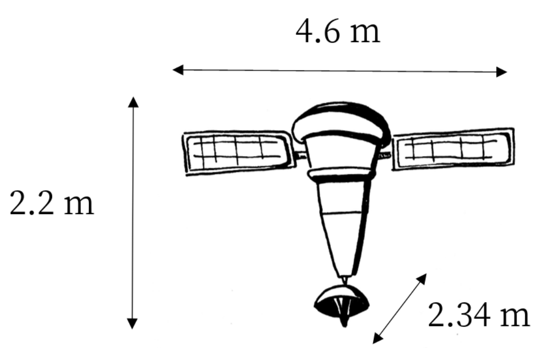

Figure 2: Schematic of CRYOSAT-2 dimensions

ENVISAT

ENVISAT is a huge satellite, its dimensions are 10 $\times$ 4 $\times$ 4 meters. Once all the tools and solar pannels (14 $\times$ 5 meters) are deployed, ENVISAT measures 25 $\times$ 7 $\times$ 10 meters ! When it has been launched, its weight was **8 140 kg** (esa, envisat). If ENVISAT is so big, it is because it aims to measure a lot of ocean, atmosphere, land and sea ice parameters at several scales. Instruments carried by ENVISAT are spectrometers, Radar Altimeter (RA-2), telescope, synthetic aperture radar and radiometer.

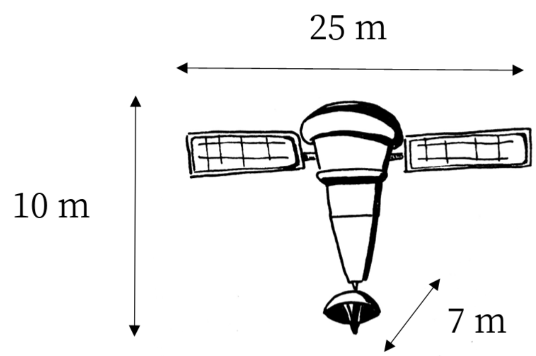

Figure 3: Schematic of ENVISAT dimensions

3.2 How do SIRAL and RA-2 altimeters work?

Figure 4 presents altimeter's functioning. Radar altimeters send wave (1) from satellite to the Earth. When the wave (1) reaches the atmosphere, one part of it is reflected (3), and the other part is transmitted (2). The transmitted part of wave (1), wave (2), then reaches the Earth surface (land or ocean), and one part of it, wave (4), will be reflected toward the satellite. Depending on whether the surface is ocean or land, the properties of the wave (4) change. **Properties of reflected wave give data about the nature of the surface. The time taken by wave (1) to reach a surface and come back to the satellite, by reflection on the surface, provides the height of the surface.**
SIRAL uses a single frequency Ku-band, whereas RA-2 pulses two waves : one at 13.575 GHz (Ku-band) and an other 3.2 GHz (S-Band). Ku-band are microwaves from 12 Gigahertz (GHz) to 18 GHz, and S-band defines electromagnetic spectrum from 2 GHz to 4 GHz.

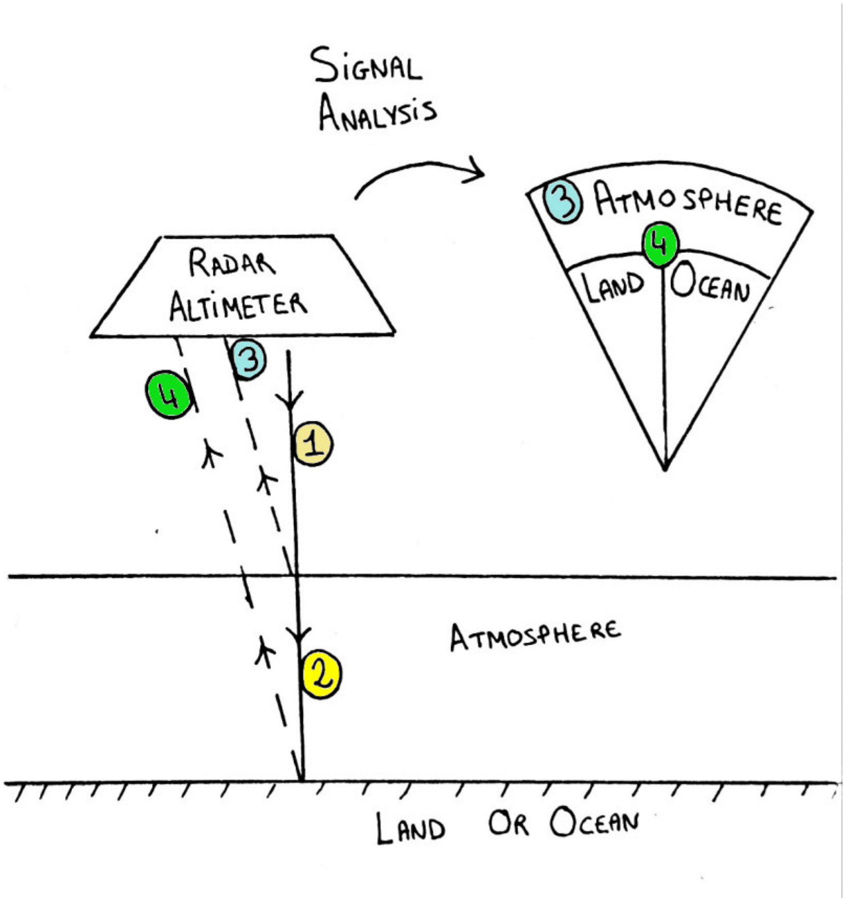

Figure 4: Schematic of radar altimeter functioning.
Wave (1) is send by the satellite. When the wave (1) is in contact with the atmosphere, one part is reflected toward the satellite (wave (3)) and an other is transmitted (wave (2)). When wave (2) reaches the surface of the Earth, one part of it is reflected toward the satellite (wave (4)).

4 GRACE : Eustatic height

4.1 How does GRACE work?

The Gravity Recovery and Climate Experiment (GRACE) has been mapping changes of the Earth's surface mass distribution since its launch in 2002. It is the main way to globally quantify underground water nowadays. GRC Tellus JPL Release-05 gridded GRACE ocean mass products has been used. **Ocean mass anomaly are provided in centimeters** of water height equivalent, from April 2002 to December 2017. Release-06 gridded GRACE data have been smoothed with a 500 km radius Gaussian filter. Data are monthly averaged.

How does GRACE work?

It is composed by two satellites, GRACE-1 and GRACE-2, flying 500 km above the Earth, and spaced by 220 km (NASA, Grace).

The twin satellites measure the distance between them, thanks to a laser on GRACE-1. This measurement is so precised that a motion of one human hair can be detected !

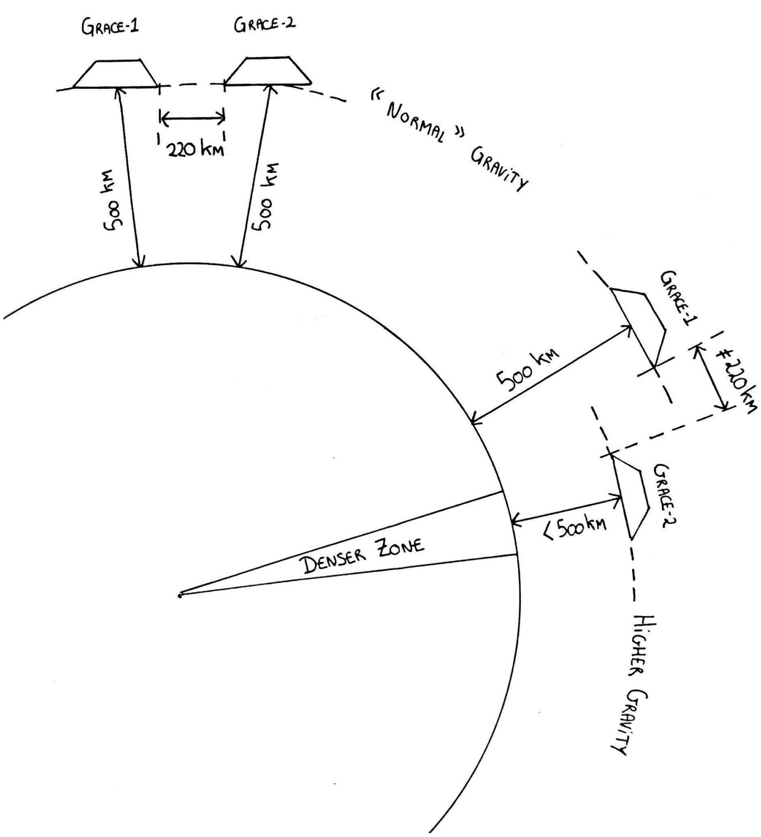

When one satellite, GRACE-2 on fig. 5, flies above a denser area, it experiences a greater gravity field : the satellite is more attracted by the Earth than the other satellite. Therefore, the distance between the twins satellite changes.
By measuring this change, the mass of the zone can be known.

Figure 5: Schematic of GRACE functioning

4.2 GRACE's limits

However, GRACE measurements have huge errors near coastal regions. An area where there is land and water is difficult to interpret for GRACE. To deal with it, a Coastline Resolution Improvement (CRI) filter has been developed (Wiese and al., 2016). Using this filter, errors near the coastline decrease by 50 %. Figure 6 presents the number of iterations required for the CRI filter. **The more iterations are required by the CRI filter, the more important is the GRACE error** (Wiese and al., 2016). Then, we expected to have important errors near the Antarctica Peninsula (longitude ≈ 60W, latitude ≈ 70S).
To know how the CRI filter works, see the Appendix "CRI filter".

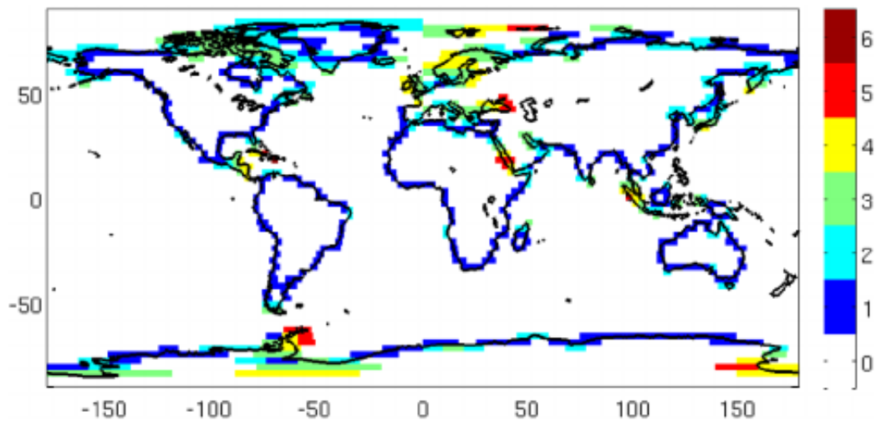

Figure 6: Number of iterations required for the CRI filter (Wiese and al., 2016)

5 ERA 5 Reanalyses: Mean Sea Level Pressure

As the weight of the atmosphere changes the height of the ocean, the weight of the air column above the ocean needs to be removed. The weight of the atmosphere above the ocean is the pressure at the sea surface.
To remove the sea surface pressure, ERA5 Reanalyses data are used. ERA5 Reanalyses provides the **Mean Sea Level pressure (MSL)** in pascal, monthly averaged. ERA5 Reanalyses provide a numerical description of the recent climate by **combining models with observations** (ECMWF).
As what we are looking for a height, **MSL needs to be converted in centimeters**. Note that as steric and eustatic height are expressed in centimeters of equivalent waters, MSL need to be converted from pascal to centimeters of equivalent water. How? It is possible, knowing a fluid pressure and density, to compute its height. (Armitage and al., 2016):

$$MSL_{[cm]} = 10^2 \frac{MSL_{[Pa]}}{\rho_0 g} \tag{1}$$

where $\rho_0 = 1028 kg.m^{-3}$ and $g = 9.81 m.s^{-2}$.

6 Joining the data together

Each satellite has its own spatial and temporal grid size. **The grid size of a satellite is how the satellite maps the Earth**. Table 1 presents the spatial and temporal resolution for each satellite database used.

Spatial resolution

Each satellite has its own spatial resolution. Spatial resolution can be indicated in degrees or in meter. All the data have been transformed in a 0,5° x 0,5° grid, as the GRACE data.

Temporal resolution

All the satellites used provide monthly averaged data. To compare the data, the time coverage taken for each data is from July 2002 to December 2017.

Data anomalies computation

GRACE data do not provide the eustatic height, but the eustatic height anomaly. Therefore, the anomaly of each data must be computed before comparing them with GRACE data. Moreover, the anomaly computation must be done as in GRACE. Eustatic height anomaly is computed in two step: (1) calculate the mean between the first day of January 2004 to the last day of December 2009 (2) anomalies are anomalies are relative to the 2004 - 2009 time-mean baseline (NASA, Grace).

Satellite	Spatial resolution	Temporal resolution
GRACE	0.5° latitude × 0.5° longitude	Apr 2002 to Dec 2017
ERA5	0.25° latitude × 0.25° longitude	1979 to Nov 2020
Cryosat/Envisat	0.5° latitude × 1° longitude	July 2002 to Oct 2018

Table 1: Satellite data details

A spatial resolution of 0.5° latitude × 0.5° longitude means that the satellite measures one value for a square of height 0.5° latitude and length 0.5° longitude.

Missing values

After 2011, there are some area where GRACE values are missing, cf white areas on figure 7. For each longitude of a bloc of missing values, a linear interpolation has been done. Linear interpolation is then done between the steric height anomalies at latitudes of the extreme locations of the bloc of missing values. Figure 8 presents the steric height anomaly after the linear interpolations.

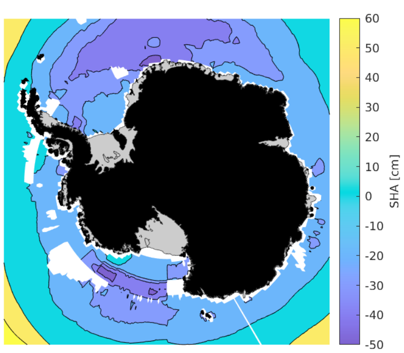

Figure 7: Steric height anomaly monthly averaged of August 2017

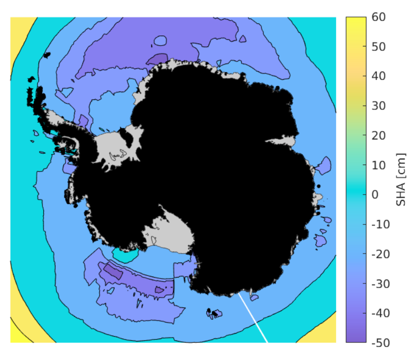

Figure 8: Steric height anomaly monthly averaged of August 2017 with linear interpolations

HOW TO BE SURE OF SATELLITES RESULTS?

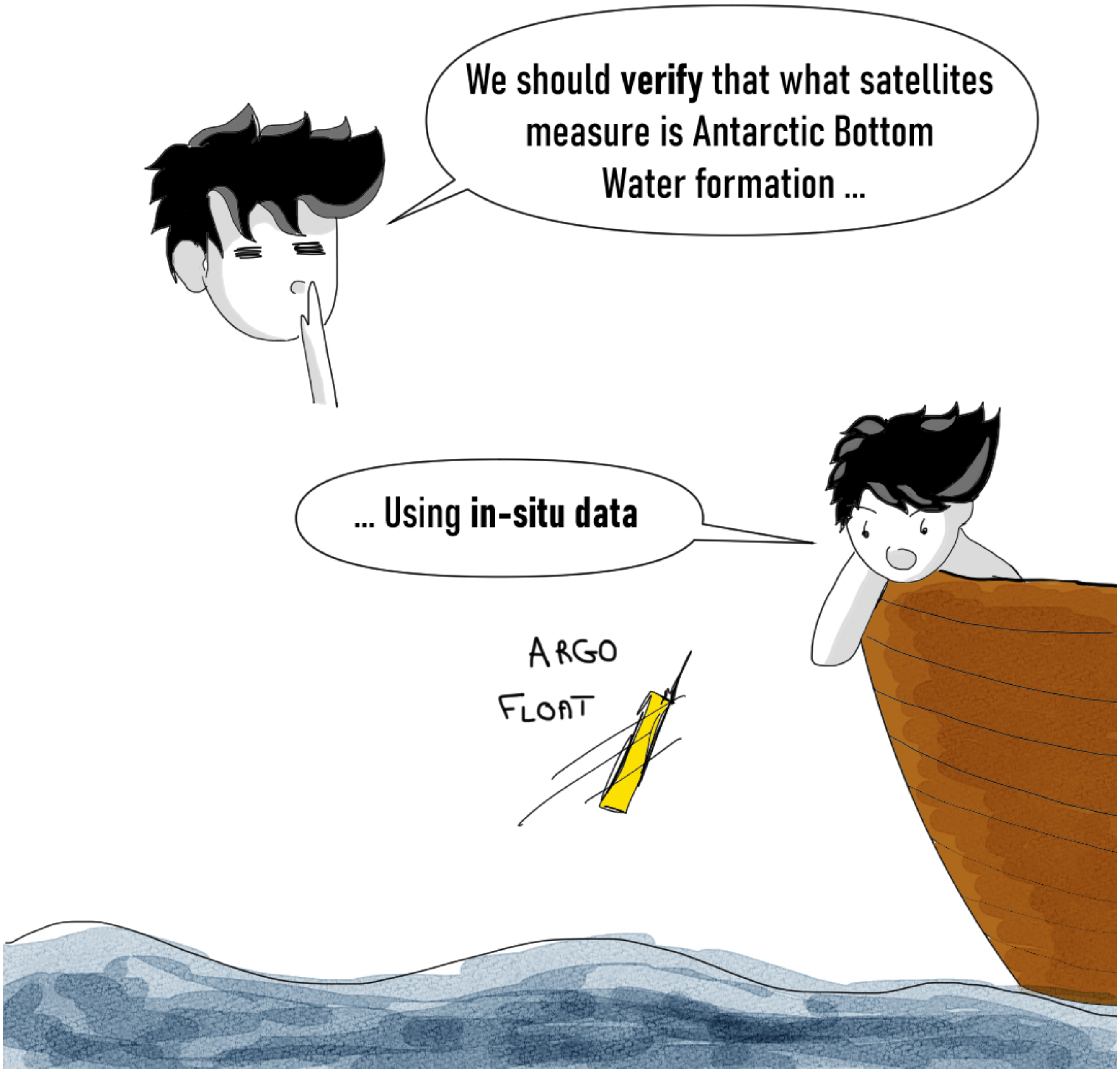

7 In-situ data

To verify that satellites provide a realistic measurement of Antarctic Bottom Water, using in-situ data is essential. Here are presented two main technologies allowing in-situ data measure ments: mooring and Argo floats. In this document, argo floats are used to identify what satellites succeed to measure. Mooring is used to verify if the evolution of the steric height anomaly in time is correct or not.

7.1 Argo float

7.1.1 Presentation

Thanks to Argo floats, ocean profiles can be known. **A profile is the evolution of one field**, such as temperature or salinity, **as a function of depth**. An example of temperature and salinity profile is presented on the graph on the right in the figure 9. From a boat, the Argo float is put in the ocean. Once in the ocean, the float moves with the currents.

7.1.2 Float cycle

The float makes a cycle (see fig. 9):
- it sinks at 1 000 meters;
- each 10 days, the float sinks at a depth between 2 000 and 6 000 meters;
- float slowly reaches the surface of the ocean, where data collected are transmitted to the satellite;
- Float begins a new cycle.

7.1.3 Argo floats used

As explained in the part I of this document "Part I: General knowledge", Weddell and Ross seas are important places for Antarctic Bottom Water formation. Therefore, 23 Argo floats in the **Weddell gyre**, 7 Argo floats in the **Ross shelf**, and 1 float in **Ross Gyre** are used for this work.
The Appendix "Argo floats used" details those floats.

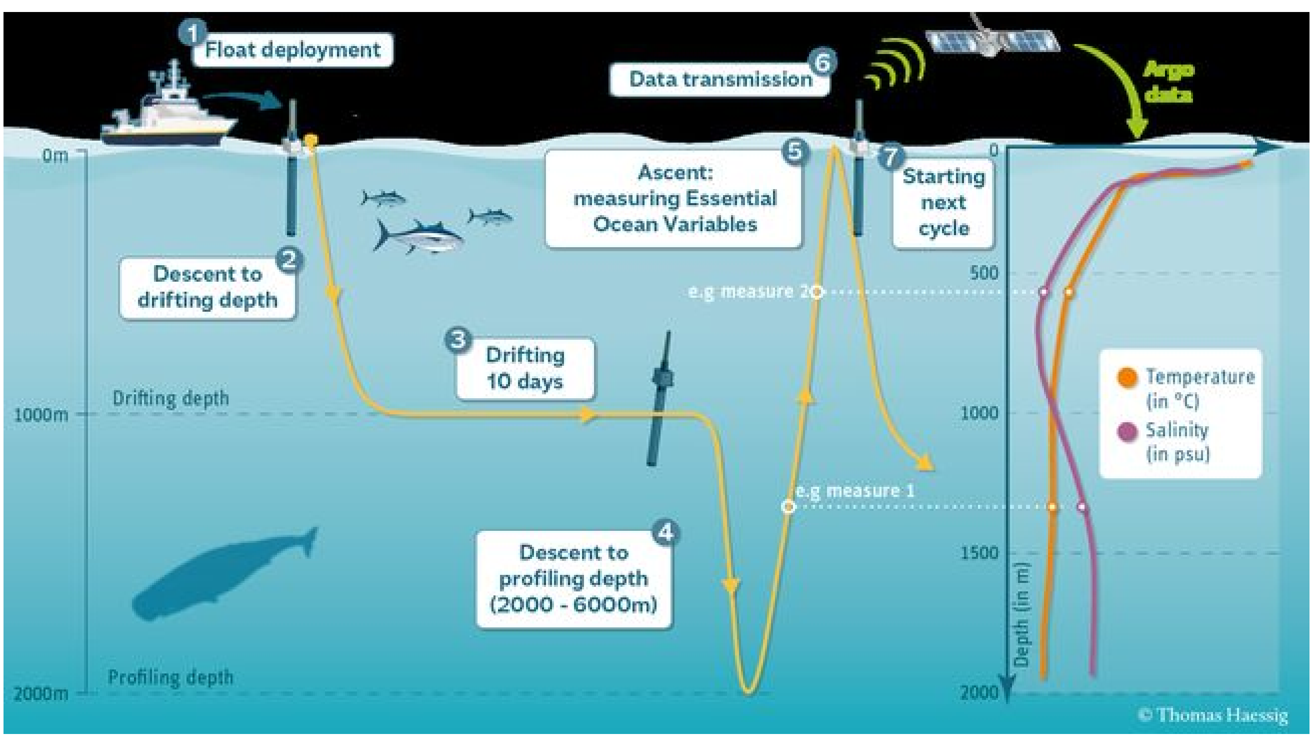

Figure 9: Argo float cycle (Euro-Argo ERIC)

7.2 Mooring

7.2.1 Presentation

A mooring is a system which measures profiles, such as temperature and salinity profiles. The difference between a mooring and one Argo float is that **Argo float drifts with currents** whereas a **mooring does not move on latitude and longitude: it is at one fixed point**. Then, as Argo floats, mooring go deeper in the ocean and come back to the upper ocean. Moorings collect data at fixed points for multiple months.

7.2.2 Mooring used

Mooring used were at longitude -116.358 °E and latitude -72.468 °N (West Antarctica, see fig. 10) from 2011 to 2016.

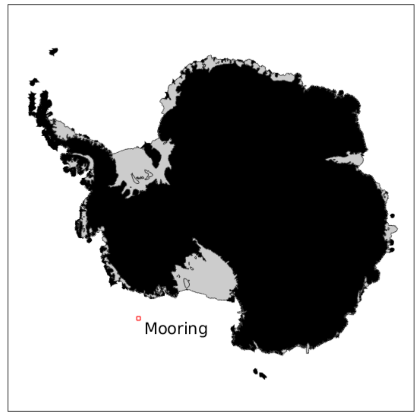

Figure 10: Location of the mooring used.
Black area is Antarctica and grey areas are ice shelves.

7.3 How to compute steric height anomaly with in-situ data?

In-situ data provide temperature, salinity and pressure. With that, it is possible to compute an **approximation of the steric height anomaly**. This approximation is called **Geopotential height**. To know its anomaly, specific volume (inverse of the density) are computed thanks to in-situ data:

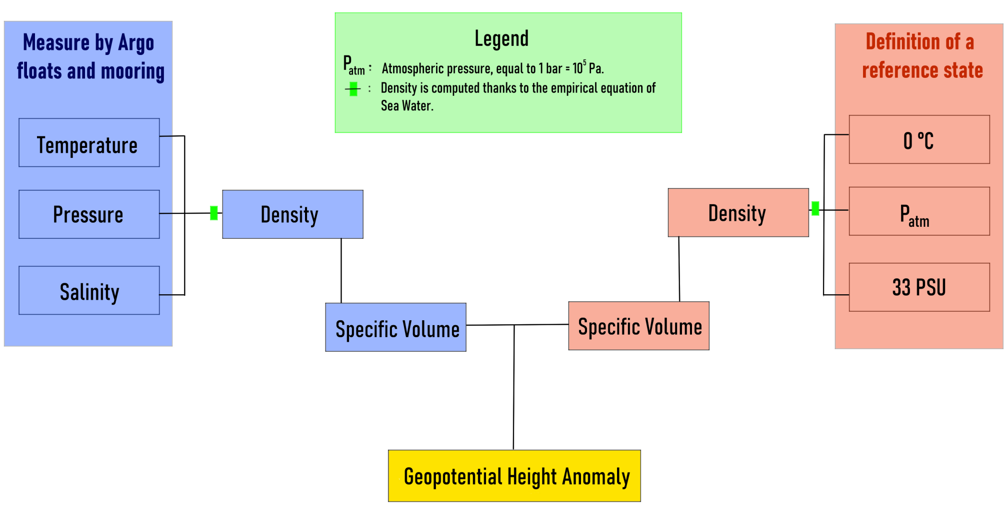

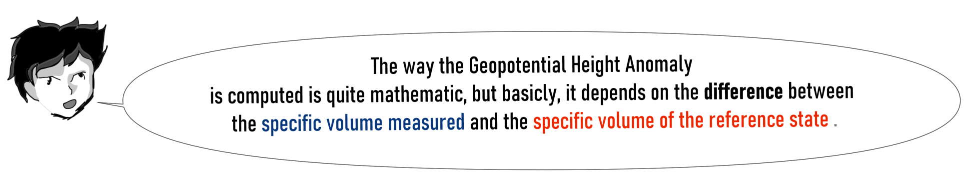

The way Geopotential Height Anomaly (GPHA) is computed is detailed in the Appendix "Geopotential height".

8 Low-pass filter on steric height anomaly

8.1 Why is a low-pass filter implemented?

What is studied here is the evolution of the Antarctic Bottom Water formation on a large time scale. It means that the variation of AABW formation from one month to another is not a matter of interests. The low-pass filter is then used to remove variations that occur with a period inferior at 6 months.

8.2 What is a low-pass filter?

In a low pass filter, a cutoff frequency f_c is defined. In theory, all the variations with a frequency smaller than f_c will be removed. In practice, **frequencies outside a pass-band frequencies will be attenuated**. Figure 11 presents a schematic of the low-pass filter functioning.

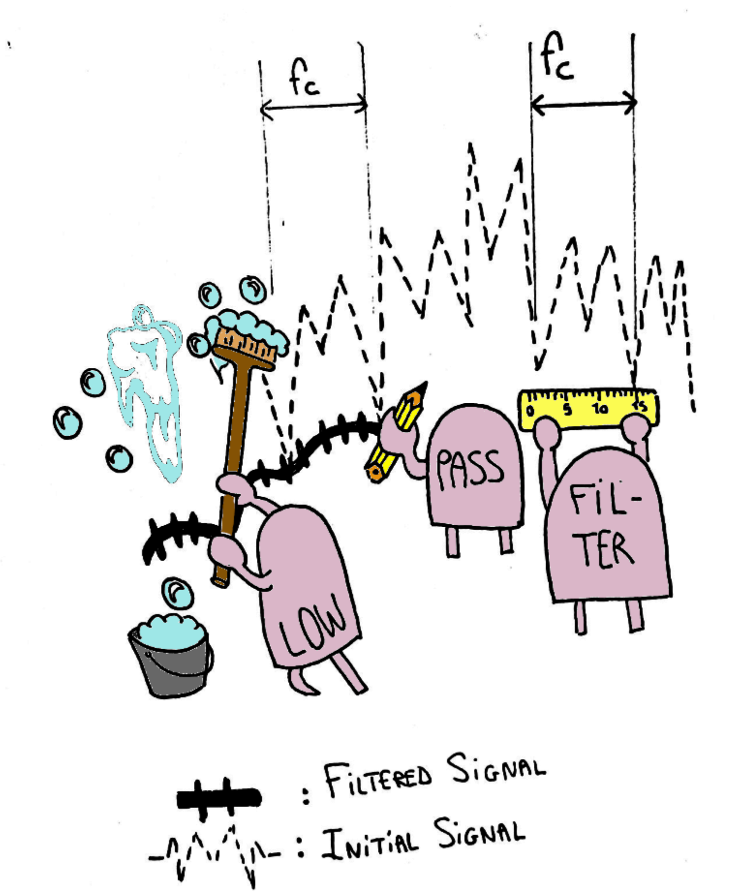

Figure 11: Schematic of low-pass filter functioning.

8.3 Low pass filter applied

As previously said, variations with a frequency of few months need to be removed. Therefore, the pass-band will be frequencies between 6 months and 2 years. In other words, only frequencies between 6 months and 2 years are considered.

Calcul of the pass-band frequencies

The period T = 6 months $\approx$ 6 months $\times$ 30 days $\times$ 24 hours $\times$ 3600 seconds $\approx$ 15 552 000 sec. The frequency is : $f_{6months} = 1/T_{6months} \approx 6 \times 10\mathrm{e}^{-8} Hz$.

The period T = 2 years $\approx$ 24 months $\times$ 30 days $\times$ 24 hours $\times$ 3600 seconds = 62 208 000 sec. The frequency is : $f_{24months} = 1/T_{24months} \approx 10\mathrm{e}^{-8} Hz$.

Figure 12a presents the filter details. Note that the magnitude is plot with a logarithmic scale. The magnitude shows if a frequency is attenuated or not. The more negative is the magnitude, the more attenuated is this frequency. On the opposite, the more positive is the magnitude, the more is considered this frequency. Using this filter, the magnitude is maximum, equal to +30 dB, for frequencies between 10e-8 Hz and 6 $\times$ 10e-8 Hz, the pass-band frequencies. Other frequencies are attenuated. Finally, the difference between satellites results with the filter applied and without the filter applied is presented on fig. 12b. Satellites results can now be compared with Argo floats!

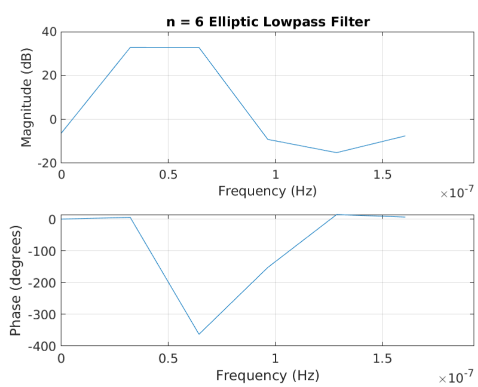

(a)

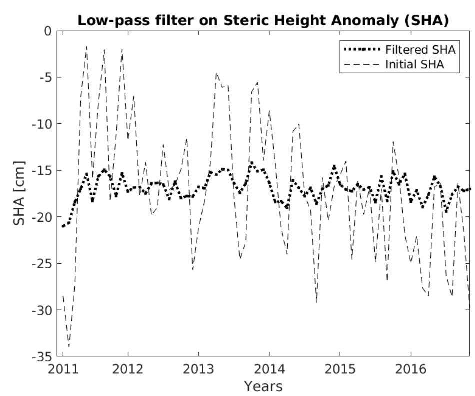

(b)

Figure 12: Low pass filter applied on steric height anomaly measured by satellites. (a) Filter details. (b) Steric height anomaly measured by satellites with and without the filter at -116.25°E and -72.75S (close to the mooring location on fig. 10).

9 Conclusion

A method using satellite data has been designed to measure antarctic bottom water formation. Antarctic bottom water formation is visible through the **steric height**. Three data sets are combined to measure steric height anomaly : eustatic height anomaly (GRACE data), mean sea level pressure (ERA5 data) and the total height of the ocean (Cryosat and Envisat data). To measure only the long-term variations of SHA, a low-pass filter has been implemented on it. In order to know if this method works or not, comparisons with in-situ data (Argo floats and mooring) must be made. These comparisons will be presented in the third part of this document: "Formation of Antarctic Bottom Water Formation, Part III: Results"!

A CRI filter

The CRI filter solves the equation 2 :

$$H_T A_T = H_L A_L + H_O A_O \tag{2}$$

where H_T is the observed total water column height of a specific GRACE spatial grid point. H_L and H_O are the parameters to solve for: the water column height of the land (L) and ocean (O) portions of the GRACE grid point. Furthermore, A_T is the total area of one GRACE grid point,A_L is its land area portion and A_O its ocean area portion.

There are more unknown (H_O and H_L) than observations (H_T) in equation 2. Therefore, the system is supplement with external a priori information. The system is then solved using batch weighted least squares (Tapley and al. 2004b), cf equation 3 and 4 :

$$(H^T W H + \overline{P}_o^{-1})\hat{x}_o = H^T W y + \overline{P}_o^{-1}\overline{x}_o \tag{3}$$

$$\hat{x}_0 = \begin{pmatrix} H_L \\ H_O \end{pmatrix}; \overline{x}_o = \begin{pmatrix} \overline{x}_L \\ \overline{x}_O \end{pmatrix}; \overline{P}_o = \begin{pmatrix} \sigma_L^2 & 0 \\ 0 & \sigma_O^2 \end{pmatrix}; y = H_T; W = \frac{1}{\sigma_{obs}^2} \tag{4}$$

where H is a matrix of partial derivatives relating the observations (y) to the state parameters ($\hat{x}_o$). W is a weighting factor on the observation, and $\overline{(}x)_o$ is an a priori estimate of the state while $\overline{P}_o$ contains variance information for $\overline{x}_o$. $\overline{x}_L$ and $\overline{x}_O$ are the a priori estimates for H_L and H_O. σ_L and σ_O represents a priori variance information for $\overline{(}x)_L$ and $\overline{(}x)_O$. Finally, σ_{obs} represents uncertainty information on the observation.

How reasonable values for $\overline{x}_O$, $\overline{x}_L$, σ_L and σ_O are selected?

For each GRACE grid point i,$\overline{x}_L$ is chosen such that it is the average water column height (area weighted) of all nearby "land" (from j=1 ...$_{NL}$) of the grid point i, within a radius D (equation 5). Similarly, $\overline{x}_O$ is chosen such that it is the average water column height (area weighted) of all nearby "ocean" (from k=1 ...$_{NO}$) grid point i, within a radius D (equation 5). Several values of D have been tested, and Wiese and al. 2016 have found that results were not overly sensitive to this parameter. Then, D has been empirically chosen equal to 640 km.

The uncertainties (equations 6) on the a priori estimates for a given GRACE grid point are calculated using a time series (from t=1... N_t) of both the Global Land Data Assimilation System (GLDAS) land surface hydrology model NOAH (Rodell and al., 2004) and the Estimating the Circulation and Climate of the Ocean, Phase 2 (ECCO2) ocean model (Menemenlis and al., 2008), both represented at 1° spatial resolution.

$$\overline{x}_L^i = \sum_{N_L, j=1} \frac{H_L^j A_L^j}{\sum_{N_L, j=1} A_L^j} \qquad \overline{x}_O^i = \sum_{N_O, k=1} \frac{H_O^k A_O^k}{\sum_{N_O, k=1} A_O^k} \tag{5}$$

$$\sigma_L^i = \sqrt{\frac{\sum_{N_t, t=1}(\hat{x}_L^{GLDAS} - \overline{x}_L^{GLDAS})}{N_t}} \qquad \sigma_O^i = \sqrt{\frac{\sum_{N_t, t=1}(\hat{x}_O^{ECCO2} - \overline{x}_O^{ECCO2})}{N_t}} \tag{6}$$

B Geopotential height

B.1 What is the Geopotential height?

The geopotential Φ is defined as :

$$\Phi(h) = \int_0^h g(\phi, z)dz \tag{7}$$

where h is the elevation above the sea surface, ϕ is the latitude and $g(\phi, z)$ the gravity at latitude ϕ and height z. The geopotential height, in meter, is :

$$GPH(h)_m = \frac{\Phi(h)}{g_0} \tag{8}$$

where g_0 is the standard gravity equal to 9.81 $m.s^{-2}$.
To use the density, and the gravity in equation 7, the following relation is used :

$$p(\phi, z) = p_{atm} - \rho(\phi, z)g(\phi, z)z \tag{9}$$

$$\Rightarrow \frac{dp}{dz} = -[\frac{\partial \rho}{\partial z}gz + \frac{\partial g}{\partial z}\rho z + \rho g] \tag{10}$$

where p_{atm} is the atmospheric pressure at the surface, equal to 1 bar.
If z=1 km, $\Delta z = -1kmm$, $gz \approx= -10^4 m^2.s^{-2}$ and ρ varies of $+0.1kg.m^{-3}$, then : $\frac{\Delta\rho}{\Delta z} = -10^{-4}kg.m^2$.
If z=1 km, $\Delta z = -1km$, $\rho z \approx -10^4 kg.m^{-2}$ and g varies of $-0.1m.s^{-2}$, then : $\frac{\Delta g}{\Delta z} = +10^{-4}s^{-2}$.
Hence, $\frac{\partial \rho}{\partial z}gz \approx +1$ and $\frac{\partial g}{\partial z}\rho z \approx -1$. Equation 10 can be re-write :

$$\frac{dp}{dz} = -\rho g \Rightarrow dp = -\rho g dz \tag{11}$$

$$\Phi = -\int_{p(0)}^{p(h)} \frac{1}{\rho}dp \tag{12}$$

Then, the geopotential height is :

$$GPH(p(h))_m = -\int_{p(0)}^{p(h)} \frac{1}{\rho g_0}dp \tag{13}$$

If h is positive, the boundaries of the integral need to be inverted because p(h) is inferior at $p(0) = p_{atm}$ (equation 14). If h is negative, the boundaries of the integral are in the right order, and equation 13 is used.

$$GPH(p(h))_{m,h>0} = +\int_{p(h)}^{p(0)} \frac{1}{\rho g_0}dp \tag{14}$$

Nota bene : Calcul of Δg
g is proportional to $\frac{1}{R^2}$, R is the Earth radius.
If the Earth radius R decreases of 1 km (dR = - 1 km), then :

$$\Delta g = g(R) - g(R - dR) = Gm_E[\frac{1}{R^2} - \frac{1}{(R-dR)^2}] = Gm_E[\frac{dR^2 - 2RdR}{R^2(R-dR)^2}] \approx 10^{-1}m.s^{-2} \tag{15}$$

where $R \approx 10^6 m$, $R - dR \approx 10^6 m$, $G \approx 6.10^{-11} m^3.kg^{-1}.s^{-2}$ is the gravitational constant and $m_E \approx 6.10^2 4kg$ is the mass of the Earth.

B.2 How is Geopotential height anomaly computed with ARGO?

Argo provides, among others, vertical profiles of temperature, salinity and pressure. With this parameter, the density of the water is computed using the equation of Seawater. The equation of Seawater is an empirical nonlinear thermodynamic relationship, see equation 18.
Then, the specific volume anomaly δ is calculated as:

$$\delta = v_S(S,T,p) - v_S(35,0,p) \tag{16}$$

where $v_S(S,T,p) = \rho(S,T,p)^{-1}$ is the specific volume at temperature T, salinity S and pressure p (Gills 1982). g_0 is the standard gravity equal to 9.81 $m.s^{-2}$.Finally, the GeoPotential Height anomaly (GPHA) is :

$$GPHA_{[cm]} = 10^2 \int_0^{p_0} \frac{\delta}{g_0} dp \tag{17}$$

.

$$\rho(S,T,p) = \frac{\rho(S,T,0)}{1 - p/K(S,T,p)} \tag{18}$$

with :

$$\begin{aligned}
\rho(S,T,0) &= 999.842594 + 6.793952 \times 10^{-2}T - 9.095290 \times 10^{-3}T^2 + 1.001685 \times 10^{-4}T^3 \\
&- 1.120083 \times 10^{-6}T^4 + 6.536332 \times 10^{-9}T^5 + 8.24493 \times 10^{-1}S - 4.0899 \times 10^{-3}TS \\
&+ 7.6438 \times 10^{-5}T^2S - 8.2467 \times 10^{-7}T^3S + 5.3875 \times 10^{-9}T^4S - 5.72466 \times 10^{-3}S^{3/2} \\
&+ 1.0227 \times 10^{-4}TS^{3/2} - 1.6546 \times 10^{-6}T^2S^{3/2} + 4.8314 \times 10^{-4}S^2
\end{aligned}$$

$$\begin{aligned}
\text{K(S,T,p)} &= 19652.21 + 148.4206\text{T} - 2.327105\text{T}^2 + 1.360447 \times 10^{-2}T^2 \\
&- 5.155288e - 5 \times 10^{-5}T^4 + 3.239908p + 1.43713 \times 10^{-3}pT + 1.16092 \times 10^{-4}t^2p \\
&- 5.77905 \times 10^{-7}pT^3 + 8.50935 \times 10^{-5}p^2 - 6.12293 \times 10^{-6}Tp^2 + 5.2787 \times 10^{-8}p^2T^2 \\
&+ 54.6746S - 0.603459TS + 1.09987 \times 10^{-2}T^2S - 6.1670 \times 10^{-5}T^3S \\
&+ 7.944 \times 10^{-2}S^{3/2} + 1.6483 \times 10^{-2}TS^{3/2} - 5.3009 \times 10^{-4}T^2S^{3/2} + 2.2838 \times 10^{-3}pS \\
&- 1.0981 \times 10^{-5}pTS - 1.6078 \times 10^{-6}pT^2S + 1.91075 \times 10^{-4}pS^{3/2} - 9.9348 \times 10^{-7}p^2S \\
&+ 2.0816 \times 10^{-8}p^2TS + 9.1697 \times 10^{-10}p^2T^2S;
\end{aligned}$$

C Argo floats used

C.1 In the Weddell Gyre

23 Argo floats in the Weddell Sea are used in this work. They are all located in the **Weddell gyre**. Table 2 presents the details of these floats.

Argo float	W number	2014-2015 First - End	2015-2016 First - End	2016-2017 First - End	2017-2018 First - End
1	5904472	-	-	3 Oct - 30 Dec	5 Jan - 10 Jan 2018
2	7900310	-	-	-	20 Jun - 12 Jan 2018
3	7900364	25 Jan - 14 Apr	-	-	-
4	7900365	22 Aug - 30 Dec	10 Jan - 5 Feb	-	-
5	7900367	25 Jan - 4 Apr	-	-	-
6	7900370	20 Jan - 7 Jul	-	-	-
7	7900372	19 Jan - 8 May	-	-	-
8	7900373	16 May - 23 Dec	3 Jan - 12 Mar	-	-
9	7900374	-	16 Jan - 8 Dec	-	-
10	7900376	24 Jan - 21 Dec	1 Jan - 5 Feb	-	-
11	7900377	16 Jan - 25 Mar	-	-	-
12	7900378	24 Jan - 4 Mar	-	-	-
13	7900379	20 Jan - 9 Apr	-	-	-
14	7900381	26 Mar - 22 Dec	2 Jan - 11 Feb	-	-
15	7900382	17 Jan - 7 Mar	-	-	-
16	7900383	20 Jan - 9 Apr	-	-	-
17	7900413	11 Feb - 10 Mar	-	-	-
18	7900464	-	-	-	11 Feb - 14 Jan 2018
19	7900467	-	-	-	3 Feb - 13 Aug 2017
20	7900471	-	-	-	7 Feb - 19 Apr 2017
21	7900472	-	-	-	1 Feb - 12 Nov 2017
22	7900473	-	-	-	7 Feb - 4 Jul 2017
23	7900492	-	-	-	1 Feb - 15 Jan 2018

Table 2: Argo floats used in Weddell Sea

C.2 In the Ross Shelf

7 Argo floats in the Ross Sea are used in this work. They are all located in the **Ross shelf**. Table 3 presents the details of these floats.

Argo float	W number	2013-2014 First - End	2014-2015 First - End	2015-2016 First - End	2016-2017 First - End
1	5904150	21 Dec - 28 Feb	28 Dec - 7 Mar	21 Dec - 29 Feb	19 Dec - 12 Mar
2	5904152	21 Dec - 14 Feb	27 Nov - 11 Mar	19 Dec - 19 Feb	18 Dec - 25 Feb
3	5904163	21 Dec - 7 Jan	11 Jan - 8 Mar	22 Dec - 29 Feb	6 Dec - 13 Mar
4	5904165	21 Dec - 21 Jan	7 Jan - 3 Mar	25 Dec - 26 Feb	27 Nov - 19 Mar
5	5904166	21 Dec - 28 Feb	3 Jan - 7 Mar	21 Dec - 28 Feb	12 Dec - 13 Mar
6	5904167	21 Dec - 15 Jan	18 Jan - 7 Mar	22 Dec - 22 Feb	21 Nov - 20 Mar
7	5904168	21 Dec - 28 Feb	10 Jan - 7 Mar	21 Dec - 28 Feb	13 Dec - 13 Mar

Table 3: Argo floats used in Ross Sea

C.3 In the Ross Gyre

1 Argo float in the Ross Gyre is used in this work. Table 4 presents the details of this float. Note that because satellite provide results until December 2017, only float's results until this date are considered. In reality, this float ended the 26 April 2020.

Argo float	W number	2013-2014 First - End	2014-2015 First - End	2015-2016 First - End	2016-2017 First - End	2017-2018 First - End
1	7900336	7 Feb - 24 Dec	3 Jan - 19 Dec	1 Jan - 28 Dec	7 Jan - 25 Dec	4 Jan - 15 May

Table 4: Argo float used in Ross Gyre

References

[1] ECMWF
European Centre for Medium-Range Weather Forecasts
https://www.ecmwf.int/en/newsletter/147/news/era5-reanalysis-production

[2] Euro-Argo ERIC
European contribution to the Argo programme
https://www.euro-argo.eu

[3] esa, cryosat
European Space Agency, CRYOSAT
https://earth.esa.int/eogateway/missions/cryosat/description

[4] esa, envisat
European Space Agency, ENVISAT
https://earth.esa.int/eogateway/missions/envisat?text=envisat

[5] NASA, Grace
NASA website : https://www.nasa.gov/mission_pages/Grace/overview/index.html

[6] Wiese and al., 2016
Wiese, D. N., F. W. Landerer, and M. M. Watkins (2016), Quantifying and reducing leakage errors in the JPL RL05M GRACE mascon solution, Water Resour. Res., 52, 7490–7502, doi:10.1002/2016WR019344

Document published on Culture Sciences de l'Ingénieur : https://eduscol.education.fr/sti/si-ens-paris-saclay